

# Transcellular Neuroligin-2 Interactions Enhance Insulin Secretion and Are Integral to Pancreatic $\beta$ Cell Function\*<sup>§</sup>

Received for publication, July 12, 2011, and in revised form, April 22, 2012. Published, JBC Papers in Press, April 23, 2012, DOI 10.1074/jbc.M111.280537

Arthur T. Suckow<sup>†§</sup>, Charles Zhang<sup>‡</sup>, Sonya Egodage<sup>‡</sup>, Davide Comoletti<sup>¶1</sup>, Palmer Taylor<sup>¶</sup>, Meghan T. Miller<sup>¶</sup>, Ian R. Sweet<sup>||</sup>, and Steven D. Chesser<sup>‡2</sup>

From the <sup>‡</sup>Department of Medicine and Pediatric Diabetes Research Center, UCSD School of Medicine, the <sup>§</sup>Biomedical Sciences Graduate Program, and the <sup>¶</sup>Department of Pharmacology, Skaggs School of Pharmacy and Pharmaceutical Science, University of California, San Diego, La Jolla, California 92093 and the <sup>||</sup>Department of Medicine, University of Washington, Seattle, Washington 98195

**Background:** The synaptic protein neuroligin-2 is present on the pancreatic  $\beta$  cell surface and affects insulin secretion.

**Results:** Insulin secretion increases when  $\beta$  cells contact adjacent cells expressing neuroligin; soluble neuroligin inhibits secretion.

**Conclusion:** Clustered neuroligin-2 enhances insulin secretion in a transcellular manner, likely by promoting secretory microdomain formation.

**Significance:** Transcellular protein-protein interactions paralleling the transsynaptic interactions that drive synapse formation may guide  $\beta$  cell functional maturation.

Normal glucose-stimulated insulin secretion is dependent on interactions between neighboring  $\beta$  cells. Elucidation of the reasons why this cell-to-cell contact is essential will probably yield critical insights into  $\beta$  cell maturation and function. In the central nervous system, transcellular protein interactions (*i.e.* interactions between proteins on the surfaces of different cells) involving neuroligins are key mediators of synaptic functional development. We previously demonstrated that  $\beta$  cells express neuroligin-2 and that insulin secretion is affected by changes in neuroligin-2 expression. Here we show that the effect of neuroligin-2 on insulin secretion is mediated by transcellular interactions. Neuroligin-2 binds with nanomolar affinity to a partner on the  $\beta$  cell surface and contributes to the increased insulin secretion brought about by  $\beta$  cell-to- $\beta$  cell contact. It does so in a manner seemingly independent of interactions with neurexin, a known binding partner. As in the synapse, transcellular neuroligin-2 interactions enhance the functioning of the submembrane exocytic machinery. Also, as in the synapse, neuroligin-2 clustering is important. Neuroligin-2 in soluble form, rather than presented on a cell surface, decreases insulin secretion by rat islets and MIN-6 cells, most likely by interfering with endogenous neuroligin interactions. Prolonged contact with neuroligin-2-expressing cells increases INS-1  $\beta$  cell proliferation and insulin content. These results extend the known parallels between the synaptic and  $\beta$  cell secretory machineries to extracellular interactions. Neuroligin-2 interactions are one of the

few transcellular protein interactions thus far identified that directly enhance insulin secretion. Together, these results indicate a significant role for transcellular neuroligin-2 interactions in the establishment of  $\beta$  cell function.

Cell-to-cell contact between pancreatic  $\beta$  cells is essential for normal glucose-stimulated insulin secretion (1, 2). The resulting interactions enable a robust secretory response to glucose, enhance suppression of insulin release at basal conditions, and facilitate  $\beta$  cell maturation (1–3). Little is known, however, about why this is so (1). In contrast to the very large body of work concerning the intracellular signaling pathways and protein machinery controlling insulin secretion by  $\beta$  cells, only two transcellular interactions that play a direct role in normal insulin secretion have been identified. The first is the coupling of adjacent  $\beta$  cells by connexin36 channels (1, 4, 5). The gap junctions thus formed decrease basal secretion and enable the intrainlet synchronization of insulin release necessary for normal glucose-stimulated insulin secretion (4, 6). A second transcellular interaction involving ephrin-A5 and EphA5 directly affects both basal and stimulated insulin secretion (7). E-cadherin and neural cell adhesion molecule are also expressed by  $\beta$  cells and engage in extracellular interactions; these help mediate the establishment of normal islet architecture (1, 8, 9). Although alterations in expression of neural cell adhesion molecule and E-cadherin affect insulin secretion, there are insufficient data to determine whether the observed changes are attributable to effects on transcellular interactions (8, 9).

The  $\beta$  cell insulin secretory apparatus is remarkably similar to the machinery used by neurons for neurotransmitter release. Many of the scaffolding, subplasmalemmal, and synaptic vesicle proteins important for neurotransmitter secretion are expressed by  $\beta$  cells and are key components of the insulin secretory machinery (10). In neurons, extracellular interactions between synaptogenic (synapse-inducing) synaptic adhesion

\* This work was supported, in whole or in part, by National Institutes of Health Grant R01DK080971 and Grant DK17047 (for the University of Washington Diabetes Endocrine Research Center Islet Core). This work was also supported by Juvenile Diabetes Research Foundation Grant 37-2009-44.

<sup>§</sup> This article contains supplemental Figs. S1–S4.

<sup>1</sup> Present address: Child Health Institute of New Jersey and Dept. of Neuroscience and Cell Biology, UMDNJ/Robert Wood Johnson Medical School, New Brunswick, NJ 08901.

<sup>2</sup> To whom correspondence should be addressed: Dept. of Medicine and Pediatric Diabetes Research Center, UCSD School of Medicine, 9500 Gilman Dr. MC 0983, La Jolla, CA 92093. Tel.: 858-822-6567; Fax: 858-534-1218; E-mail: schessler@ucsd.edu.

molecules on opposite sides of the synaptic cleft trigger assembly of the protein complexes necessary for neurotransmitter signaling (11). By binding and clustering their presynaptic partners, postsynaptic synaptogenic adhesion molecules, including members of the neuroligin family, induce the formation of the presynaptic machinery for regulated secretion (11). In co-culture experiments, transfected, non-neuronal cell lines expressing neuroligins induce presynaptic differentiation at points of contact with co-cultured hippocampal neurons (11–13).

Clustering on the cell surface (either in the postsynaptic membrane or, in co-culture models, in the plasma membrane of transfected cells) is necessary for neuroligins to promote synapse formation and normal neurotransmission (12, 13). The neuroligin extracellular domains alone lack synapse-inducing activity, but, when neuroligin is presented to neurons on the surface of cells or clustered on beads, assembly of presynaptic active zones of neurotransmitter release is induced at sites where the extracellular domains come into contact with neuronal processes (12, 13).

We previously found that neuroligin-2 (NL-2),<sup>3</sup> which is specific to inhibitory (GABAergic) synapses, is expressed by pancreatic  $\beta$  cells and that alterations in its level of expression affected insulin secretion by primary rat islet and INS-1  $\beta$  cells (11, 14). Increased NL-2 expression caused increased insulin secretion, and decreased expression lowered insulin secretion (14). In work done elsewhere (15), NL-2 was one of the most abundant transcripts identified in a systematic study of human tissue mRNAs that was carried out in order to identify highly expressed, human islet-specific membrane proteins.

Our prior study determined that NL-2 affects insulin secretion but did not test the mechanism of this effect, most importantly whether the increased secretion is driven by extracellular interactions (14). The central role of transcellular neuroligin interactions in synapse maturation along with the known importance of  $\beta$  cell-to- $\beta$  cell contacts in insulin secretion led us to hypothesize that the effect of NL-2 on insulin secretion is mediated by transcellular interactions. Here we demonstrate that NL-2 in clustered but not soluble form increases insulin secretory capacity in a transcellular manner. Neuroligin-1 (NL-1) can similarly increase insulin secretion. Although neurexin-1 $\alpha$ , a major neuroligin binding partner, is present on the  $\beta$  cell surface, neurexin binding is not necessary in order for neuroligin to influence insulin secretion (16). In longer term experiments, transcellular NL-2 interactions increased INS-1  $\beta$  cell proliferation and insulin content. The effect of transcellular NL-2 interactions on insulin secretion occurs distal to glucose sensing. In parallel with its effects on presynaptic active zone formation and neurotransmitter exocytosis in synapses, NL-2 probably enhances insulin secretion by promoting formation and/or function of the submembrane,  $\beta$  cell insulin secretory microdomains. These data identifying transcellular NL-2 interactions as necessary for normal insulin secretion increase our understanding of why contact between  $\beta$  cells is essential to normal  $\beta$  cell function and of the role of synaptogenic adhesion molecules in the establishment of  $\beta$  cell function.

## EXPERIMENTAL PROCEDURES

**Cell Culture and Islet Isolation**—INS-1 cells were cultured in RPMI 1640 medium with 10% FBS, 50  $\mu$ M  $\beta$ -mercaptoethanol, and 1 mM sodium pyruvate (INS-1 cell medium). MIN-6 cells were cultured in DMEM with 20% FBS with 50  $\mu$ M  $\beta$ -mercaptoethanol (MIN6 medium). HEK293 cells were cultured in DMEM with 10% FBS (HEK medium). Rat islets were isolated from Sprague-Dawley rats (240–260 g; Charles River Laboratories) as described previously and cultured for 18 h to allow for recovery (14). Animal procedures were approved by the University of California, San Diego, Institutional Animal Care and Use Committee. Rat islets were cultured in RPMI 1640 with 10% FBS and 2.5  $\mu$ g/ml amphotericin B (islet medium). L-Glutamine (2 mM), 100 units/ml penicillin, and 100 mg/ml streptomycin were also added to the medium.

**Co-culture Assays**—HEK293 cells grown to 100% confluence in antibiotic-free medium were transfected using Lipofectamine 2000 (Invitrogen) in 24-well plates with full-length NL-2, with the same construct containing only the epitope tag, with neuroligin-1 (NL-1), with NL-1-G500A, or with CASPR2. All of these constructs carried N-terminal FLAG epitope tags. CASPR2 cDNA was cloned into pcDNA3.1, and the other proteins were encoded by previously described plasmids (17, 18). After 24 h, dispersed MIN-6, INS-1 or primary rat islet cells were seeded onto the transfected cells.

In some experiments, transfected HEK293 cells were, after 48 h, fixed for 10 min with 4% paraformaldehyde and washed repeatedly with PBS. The short incubation time, although lethal to cells, allows retention of protein enzymatic and binding activity (paraformaldehyde is used in a similar manner to fix *Staphylococcus aureus* with nearly complete retention of protein A binding activity) (19, 20). The fixed cell monolayers were stored in PBS at 4 °C. Dispersed INS-1 cells were cultured in contact with the fixed HEK293 cells for 24 h.

MIN6 and INS-1 co-cultures were incubated for 24 h in MIN-6 medium or in a 50/50 mix of INS-1 and HEK medium, respectively. Dispersed islet cells were prepared by gently dissociating rat islets with 0.01% trypsin, 0.1 mM EDTA in Ca<sup>2+</sup>/Mg<sup>2+</sup>-free Hanks' balanced salt solution. They were then co-cultured in a 50/50 mix of HEK and islet media at 11.1 mM glucose.

**Treatment with Soluble Neuroligin**—Recombinant soluble NL-2 with a stop codon replacing Phe-616 and recombinant soluble NL-1 with a stop codon replacing residue 639 and with or without a Gly to Ala mutation at residue 500 (G500A) (all with N-terminal FLAG epitope tags) were produced as described previously (17, 18). Soluble acetylcholinesterase was also prepared as described previously (21). Small clusters of MIN-6 cells or rat islets were washed with Krebs-Ringer bicarbonate (KRB) buffer containing 2.75 mM glucose, aliquoted to wells on a 96-well plate, and allowed to equilibrate for 45 min. Cells were then incubated in KRB buffer with 30 mM glucose (20 mM for islets) containing either a control peptide (three FLAG epitope tags in series), soluble acetylcholinesterase, or soluble NL-1 or NL-2. Cells were lysed in radioimmune precipitation assay buffer (Sigma). Secreted insulin and cellular insulin content were analyzed by radioimmunoassay (Millipore).

<sup>3</sup> The abbreviations used are: NL-2, neuroligin-2; NL-1, neuroligin-1; KRB, Krebs-Ringer bicarbonate; IBMX, 3-isobutyl-1-methylxanthine.

## Transcellular Neuroligin-2 Interactions in $\beta$ Cell Function

**Insulin Secretion**—For analyses of insulin secretion, cells were washed twice with KRB buffer containing 2.75 mM glucose and then equilibrated in this solution for 45 min. The cells were then treated for 1 h with KRB buffer containing either 2.75 mM glucose or 16.75 mM glucose (30 mM for MIN6). Where indicated, buffer was supplemented with 100  $\mu$ M IBMX to enhance stimulated insulin secretion. For analyses of  $K^+$ -stimulated insulin secretion, cells co-cultured for 24 h were washed twice with KRB buffer containing 2.75 mM glucose, next equilibrated in this solution for 45 min, and then treated with KRB buffer containing either 2.75 mM glucose, 20 mM glucose, or 30 mM KCl for 1 h. Protein was extracted with radioimmune precipitation assay buffer containing protease inhibitors. Insulin was analyzed by radioimmunoassay.

**Competitive Binding Assay**—Soluble NL-2 was labeled with  $^{125}$ I by Dr. Robert Speth (University of Mississippi radioiodination core) by the Iodogen method (Thermo Scientific). The specific activity of  $^{125}$ I-labeled soluble NL-2 was 113.7  $\mu$ Ci/ $\mu$ g. Polypropylene test tubes containing INS-1 cells ( $2.5 \times 10^5$ ) in 170  $\mu$ l of medium were placed in a shaking water bath at 37 °C for 30 min. Varying concentrations of unlabeled soluble NL-2 were added to the test tubes, followed by  $^{125}$ I-labeled soluble NL-2 (50 pM) and then a 30-min incubation. To measure binding of the  $^{125}$ I-labeled soluble NL-2 to the cells, cell-associated radioactivity was determined after separating away the unbound protein as described previously (22). The dissociation constant ( $K_d$ ) was determined from the competitive binding data in standard fashion (23).

**FACS Analysis**—To analyze Ki67 expression, cells were aspirated from the wells after treatment with 0.05% trypsin in EDTA, spun down at  $500 \times g$  for 5 min, and then washed with PBS with 1% BSA. They were then incubated at room temperature for 10 min in 4% paraformaldehyde and washed twice with 1% BSA in PBS and stored in 1% saponin with 1% BSA in PBS. Cells were stained with 1:100 guinea pig anti-insulin primary antibody (Dako) or 1:100 mouse anti-Ki67 antibody (BD Biosciences) and then 1:1000 Alexa 488 anti-guinea pig IgG secondary antibody or 1:500 Alexa 594 anti-mouse IgG antibody (Invitrogen) in 1% saponin, 1% BSA PBS. FACS analysis was performed using a Guava flow cytometry system (Millipore).

To test for cell surface expression of NL-2 and of an NL-2 binding partner, MIN-6 and INS-1 cells were grown to 100% confluence in 75-cm<sup>2</sup> flasks and then suspended in KRB buffer after detachment from the flask using Cellstripper (Mediatech) and washing in complete medium. Cells were then either incubated for 45 min at 37 °C with 700 nM 3 $\times$  FLAG peptide or 700 nM FLAG-NL-2, both preincubated with monoclonal FLAG antibody, or at 4 °C with preimmune serum or a rabbit anti-NL-2 antibody against recombinant NL-2 extracellular domain (Lampire Biological Laboratories). Next, cells were washed three times with ice-cold KRB buffer and then incubated with AlexaFluor 488 goat anti-mouse or anti-rabbit IgG for 30 min at 4 °C. Cells were washed three more times with KRB buffer and analyzed by flow cytometry using a FACSCalibur flow cytometer (BD Biosciences).

**Streptolysin-O**—Analysis of insulin secretion stimulated by direct  $Ca^{2+}$  influx after cell permeabilization with streptoly-

sin-O was performed as described previously (24, 25). Briefly, cells co-cultured for 24 h were washed with KRB buffer containing 2.75 mM glucose, equilibrated in this solution for 45 min, and then permeabilized using 3.2 units/ml streptolysin-O (Sigma) for 30 min on ice as described previously (24, 26). Cells were then washed and equilibrated with an EGTA-buffered 0.1  $\mu$ M free  $Ca^{2+}$ , 140 mM  $K^+$ -glutamate solution for 10 min at 37 °C and next incubated with the same EGTA-buffered solution with either 0.1  $\mu$ M or 10  $\mu$ M free  $Ca^{2+}$  for 15 min at 37 °C. Total protein was extracted from co-cultured cells with radioimmune precipitation assay buffer containing protease inhibitors (Sigma). Secreted and total insulin content were analyzed by radioimmunoassay.

**Imaging Analysis**—For quantitative immunofluorescence analysis of syntaxin clustering, cells co-cultured for 24 h were washed with PBS, fixed with 4% paraformaldehyde for 1 h, and washed three times with 1% BSA in PBS-Tween (PBST) prior to staining. Cells were stained with 1:500 rabbit anti-FLAG primary antibody (Sigma) to label transfected HEK293 cells and with 1:100 mouse anti-syntaxin-1A antibody (Santa Cruz Biotechnology, Inc.). After 1 h of primary antibody incubation, cells were washed three times with 1% BSA in PBST, followed by incubation with 1:2000 Alexa 488 anti-rabbit IgG secondary antibody, and 1:500 Alexa 594 anti-mouse IgG secondary antibody (both from Invitrogen). Cells were finally washed in 1% BSA in PBST followed by three washes with PBS. Analysis of syntaxin clustering was by analysis of the punctateness of syntaxin immunofluorescence (*i.e.* the syntaxin protein content at sites of clustering, as reflected by the brightness of individual puncta of syntaxin staining, evaluated by measuring the signal intensity of syntaxin-positive pixels) as has been described previously for synapsin and other secretory proteins (27–29). An illustration of the overall approach used is provided in the supplemental material (supplemental Fig. S3). Images of eight random, discrete regions within each of the wells stained were captured using an inverted Nikon Eclipse E800 fluorescent microscope and analyzed using ImagePro software (Media Cybernetics). The average intensity of Alexa 594-positive pixels and the area covered by Alexa 488-positive pixels were calculated for each image, representing, respectively, the punctateness of syntaxin expression in INS-1 cells and the degree of contact between INS-1 cells and the extracellular domains of NL-2 or CASPR2 present on the co-cultured HEK293 cells (see supplemental Fig. S3).

**Statistical Analysis**—Data are presented as means  $\pm$  S.E. Differences between quantitative data sets were analyzed by Student's *t* test. Linear regression of data from imaging analysis and analysis of slopes by F test were performed using GraphPad Prism 5 software (GraphPad Software). Generation of a standard dose-response (inhibitor *versus* response) curve using the standard slope model and calculation of the  $IC_{50}$  was also accomplished using Prism 5.  $p < 0.05$  was considered significant.

## RESULTS

**Presence of NL-2 and NL-2 Binding Partner on  $\beta$  Cell Surface**—To confirm the presence of NL-2 on the  $\beta$  cell surface (14), we incubated intact INS-1  $\beta$  cells with an antibody against the



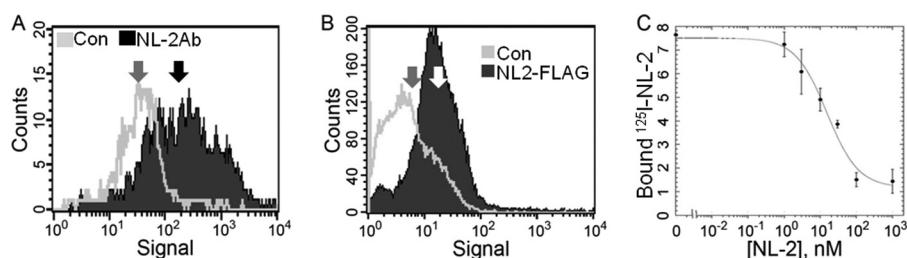


**FIGURE 1. Expression of neuroligin-2 and a binding partner on the surface of  $\beta$  cells.** *A*, INS-1 cells were incubated with an antibody against the extracellular domain of NL-2 and a fluorescent secondary antibody and then analyzed by flow cytometry. The x axis of the resulting histogram depicts the intensity of fluorescence exhibited by individual INS-1 cells. The y axis depicts the number of INS-1 cells with that intensity of fluorescence. Consistent with the presence of immunoreactive NL-2 on the surface of  $\beta$  cells, the mean of the fluorescence intensities yielded by cells treated with anti-NL-2 antibody (the mean of the filled-in curve, black arrow) was 5.5-fold greater than the mean fluorescent signal yielded by cells treated with control preimmune serum (gray arrow). *B*, soluble NL-2 extracellular domain carrying a FLAG epitope tag was incubated with INS-1 cells. Binding was assessed by incubation with an antibody against the epitope tag and a fluorescent secondary antibody and then flow cytometry. Histograms were as in *A*. Consistent with soluble NL-2 binding to the surface of  $\beta$  cells, an increase in fluorescent signal (right shift) was observed in INS-1E cells treated with soluble NL-2 (filled-in curve) relative to cells treated with a control FLAG peptide (light gray line). The mean signal intensities yielded by control-treated cells and NL-2-treated cells are depicted by gray and white arrows, respectively. *C*, to determine the affinity of NL-2 for its receptor on  $\beta$  cells, a competition binding curve was generated by incubating  $^{125}\text{I}$ -labeled soluble NL-2 tracer and varying concentrations of unlabeled soluble NL-2 with INS-1 cells. The resulting binding data yielded a  $K_d$  of 15 nM. Error bars, S.E.

extracellular domain of NL-2 and with a secondary immunofluorescent antibody. Flow cytometry was then used to detect antibody binding (Fig. 1*A*). Consistent with the presence of immunoreactive NL-2 on the INS-1  $\beta$  cell surface, the mean fluorescent signal intensity yielded by cells incubated with the anti-NL-2 antibody (the mean of the filled-in curve in Fig. 1*A*) was 5.5-fold greater than the mean signal yielded by cells treated with control, preimmune serum (the mean of the light gray curve).

Neurexins, which are known neuroligin binding partners, are also expressed by  $\beta$  cells (14, 16). To test for NL-2 binding to the  $\beta$  cell surface, flow cytometry was performed after incubating INS-1  $\beta$  cells with the extracellular domain of NL-2 (soluble NL-2). The mean fluorescent signal yielded after treatment with soluble NL-2 protein (Fig. 1*B*, white arrow) was 4.3-fold above the mean control level (Fig. 1*B*, gray arrow), consistent with specific binding of NL-2 to a partner or partners on the cell surface. Similar results were obtained with MIN-6  $\beta$  cells (data not shown). A competitive binding curve was generated to further characterize the binding of NL-2 to INS-1 cells (Fig. 1*C*). The resulting plot is consistent with a binding interaction between the NL-2 extracellular domain and a receptor on the INS-1  $\beta$  cell surface with a dissociation constant ( $K_d$ ) of 15 nM (23).

**Co-culture of  $\beta$  Cells with Cells Expressing NL-2**—To determine the effect on  $\beta$  cell function of contact with cells expressing NL-2, insulin secretion by dissociated primary rat islet cells and by dispersed MIN-6 and INS-1  $\beta$  cells was analyzed after a 24-h period of co-culture in contact with HEK293 cells transfected with full-length NL-2 or with a control construct.

MIN-6  $\beta$  cells, because of their propensity to cluster and form pseudoislets, are a proven model for investigations of the role of cell-to-cell contact in insulin secretion (2, 5). MIN-6 cells cultured on NL-2-expressing HEK293 cells secreted 2.9-fold more insulin under basal glucose conditions and 3.3-fold more insulin under stimulatory glucose conditions than MIN-6 cells co-cultured with control-transfected HEK293 cells (Fig. 2*A*). Co-culture of dispersed rat islet cells and INS-1 cells with NL-2-expressing HEK293 cells also increased insulin secretion under basal and stimulatory conditions, with stimulated insulin

secretion increasing 51 and 31%, respectively, over secretion in control co-cultures (Fig. 2, *B* and *C*).

Glucose stimulation of insulin secretion is lower in INS-1 cells and dissociated islet cells than in intact islets, and IBMX is commonly used to enhance stimulated insulin secretion (30, 31). Fig. 2*D* depicts insulin secretion in INS-1 co-cultures after stimulation with glucose alone (left two columns) or after stimulation with glucose plus IBMX (right two columns). The increases in insulin secretion induced by co-culture with NL-2-expressing cells were 77 and 82%, respectively. There was some interexperimental variability in the magnitude of the increased insulin secretion induced by NL-2. The smaller effect on basal secretion, in particular, was not always statistically significant. Differences in transfection efficiencies and perhaps cell passage numbers were likely contributors. As will be shown later, NL-1, which has high sequence homology and functional overlap with NL-2 (11, 32), similarly increases insulin secretion in a transcellular manner. Cellular insulin content, in contrast to secretion, was not affected by NL-2 after 24 h (Fig. 2*F*).

To test whether it was necessary for NL-2 to be presented by living HEK293 cells in order for there to be an effect on insulin secretion, INS-1  $\beta$  cells were cultured on monolayers of transfected HEK293 cells that had previously been fixed with paraformaldehyde (Fig. 2*E*). The fixed, NL-2-expressing HEK293 cells increased insulin secretion in contacting INS-1 cells.

**Soluble NL-2 Inhibits Insulin Secretion**—The addition of soluble, rather than clustered, forms of neuroligin or its binding partners to cultured neurons interferes with endogenous neuroligin interactions and inhibits synapse formation (12, 13, 29, 33). We next tested whether soluble neuroligin, in a parallel manner, interferes with insulin secretion. In addition to rat islets, MIN-6 cells were employed for these experiments due to their tendency to cluster into pseudoislets and their proven utility as a model for investigations of  $\beta$  cell-to- $\beta$  cell interactions (2, 5).

Clustered MIN-6  $\beta$  cells and intact rat islets were incubated with soluble NL-2 under stimulatory conditions (Fig. 3). MIN-6 cells treated with soluble NL-2 secreted 71% less insulin than cells treated with a control peptide or with soluble acetylcholinesterase, a homologous protein that lacks synaptogenic

## Transcellular Neuroigin-2 Interactions in $\beta$ Cell Function

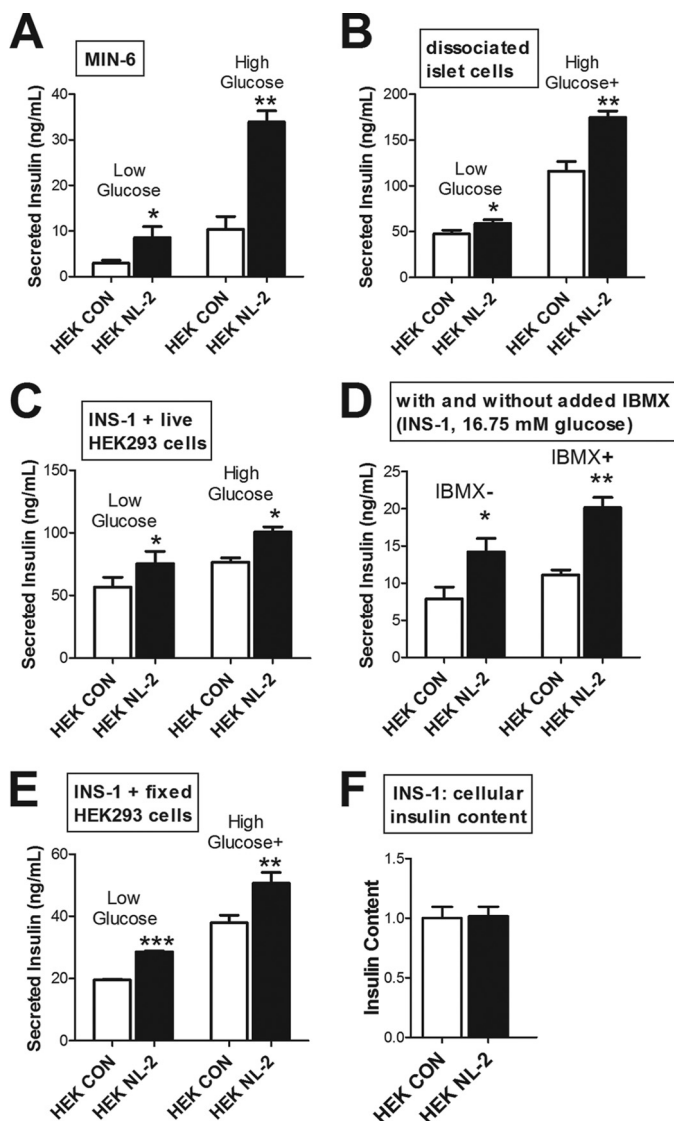


**FIGURE 2. Co-culture for 24 h of  $\beta$  cells with HEK293 cells expressing NL-2.** MIN-6 cells (A), dissociated rat islet cells (B), and INS-1 cells (C) were cultured for 24 h on monolayers of HEK293 cells transfected with either NL-2 (HEK NL-2) or with a control construct (HEK CON). Insulin secreted into the medium was measured after a 1-h incubation in low (2.75 mM) or high glucose (16.75 mM; 30 mM for MIN-6). To better observe stimulated insulin secretion, high glucose was supplemented with IBMX (100  $\mu$ M) where indicated (Glucose+). D, to compare the effect of NL-2 on INS-1 cells stimulated with either high glucose alone (IBMX-) or with high glucose plus IBMX (100  $\mu$ M; IBMX+), cells were co-cultured as in C, and insulin secretion was measured after 1 h in high glucose without (left two columns) or with IBMX (right two columns). In E, INS-1 cells were plated on HEK293 cells that had been fixed 48 h after transfection with control or NL-2 constructs and stored in PBS until use. Insulin secretion at low glucose and after stimulation with high glucose plus IBMX was measured. F, cellular insulin content was not affected by a 24-h co-culture with NL-2-expressing cells. Insulin content is shown normalized to levels in INS-1 cells co-cultured with control-transfected HEK293 cells. Results are representative of at least three separate experiments and are presented as average  $\pm$  S.E. (error bars) of 4–6 parallel replicates (\*,  $p < 0.05$ ; \*\*,  $p < 0.01$ ; \*\*\*,  $p < 0.005$ ).

activity (11, 21) (Fig. 3A). Similarly, soluble NL-2 reduced insulin secretion by rat islets (Fig. 3B). The effect on insulin secretion was dose-dependent, with maximal inhibition seen at NL-2 concentrations of 100 nM and above in Fig. 3B and the resulting inhibition curve shown in Fig. 3C.

**Effects of Longer Term Co-culture**—Co-culture experiments were repeated to determine the effect of a longer, 48-h, co-cul-

ture period. In contrast to 24-h co-culture (Fig. 2F), 48-h co-culture with NL-2-expressing HEK293 cells increased total cellular insulin in INS-1 cells (Fig. 4A) and MIN-6 cells (Fig. 4B).

The increase in cellular insulin content was further investigated in INS-1 co-cultures, which exhibited a greater increase in insulin content than co-cultures with MIN-6 cells. In the 48-h co-cultures with NL-2-expressing cells, insulin mRNA levels were increased, but so were levels of all other INS-1 cell transcripts tested (supplemental Fig. S1). INS-1 cells were counted by flow cytometry to determine if increased numbers of INS-1 cells in the NL-2 co-cultures could account for this finding. INS-1 cell numbers were greater after co-culture with NL-2-expressing cells (Fig. 4C). Indicative of increased proliferation, a greater proportion of INS-1 cells in the NL-2 co-cultures was positive for the proliferation marker Ki67 (Fig. 4D) (34). Side scatter during FACS also increased in the INS-1 cells co-cultured with NL-2-expressing cells (supplemental Fig. S1). This increase in side scatter, which could have been due to increased proliferation (35), serves as further evidence of an effect on  $\beta$  cells of contact with NL-2-expressing cells. Although INS-1 cell numbers were increased 1.5-fold in the NL-2 co-cultures (Fig. 4C), there was a 2.4-fold increase in INS-1 cell insulin content (Fig. 4A). This suggests that both INS-1 cell number and the average insulin content of each INS-1 cell were increased. This effect on proliferation was not observed with dissociated rat islet cells (not shown).

**Neurexin Binding Is Not Necessary for Increased Insulin Secretion**—Neuroigins exert effects on neural synapse formation and function through both neurexin-dependent and neurexin-independent mechanisms (36). The proteins with which neuroigins interact to mediate their neurexin-independent functions are as yet unknown (36). Because  $\beta$  cells express neurexin, primarily neurexin-1 $\alpha$ , we next asked if neurexin binding is necessary for neuroigin to cause increased insulin secretion (14, 16). Small, discrete mutations preventing the interaction of NL-2 with neurexins have not been described. In contrast, the structural basis of the interaction between NL-1 and the neurexins has been extensively characterized by mutational analysis and crystallography, and key individual NL-1 residues have been identified (18, 37, 38). The single amino acid substitution G500A involves one such residue and prevents NL-1-neurexin binding (18, 37, 38).<sup>4</sup>

Because of the high degrees of sequence homology and substantial functional overlap between NL-1 and NL-2, we reasoned that, like NL-2, NL-1 would probably also increase insulin secretion (29, 32, 39). Fig. 5A shows that, as was expected, insulin secretion is increased by co-culture of  $\beta$  cells with NL-1-expressing HEK293 cells. We next asked whether HEK293 cells expressing NL-1 with the G500A mutation (NL-1-G500A) could also increase insulin secretion. As seen in Fig. 5B, like NL-1, NL-1-G500A increased insulin secretion in co-culture experiments. We then asked whether NL-1-G500A would interfere with endogenous neuroigin interactions, decreasing insulin secretion. As before (Fig. 3B), rat islets, in which  $\beta$  cells are found in their normal three-dimensional context and native

<sup>4</sup> M. T. Miller, unpublished results.

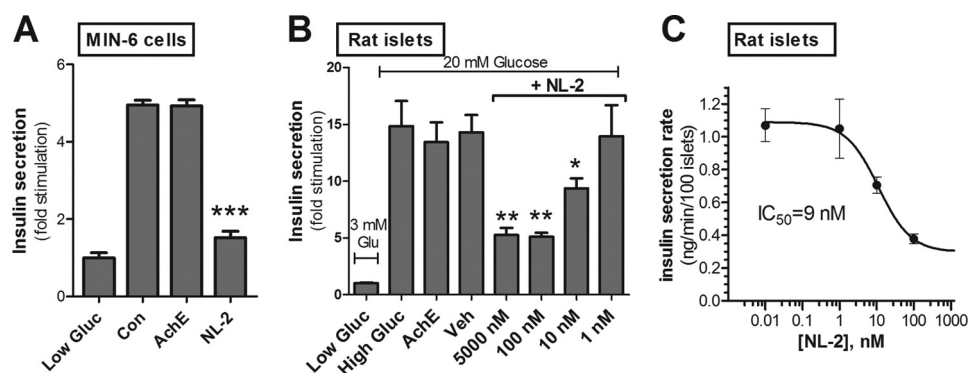


FIGURE 3. **Soluble NL-2 inhibits insulin secretion.** *A*, the effect of soluble NL-2 on stimulated insulin secretion was tested using MIN-6 cells incubated for 1 h in high glucose (30 mM). The first column on the left shows insulin secretion in low (3 mM) glucose. The other three columns represent insulin secretion at 30 mM glucose. The following were present in the media during the incubation: control peptide (*Con*; 10  $\mu$ M), soluble acetylcholinesterase (*AchE*; 10  $\mu$ M), and soluble NL-2 extracellular domain (*NL-2*; 10  $\mu$ M). Insulin secreted into the medium was measured by radioimmunoassay and is shown as -fold stimulation over unstimulated (low glucose) secretion. *B*, intact islets were conditioned for 1 h in 3 mM glucose KRB buffer and were then incubated for 1 h in low (3 mM; column on far left) or in high (20 mM) glucose along with, from left to right on the graph, no additive (second column from left), 5  $\mu$ M soluble acetylcholinesterase (*AchE*; third column from left), and NaCl-HEPES vehicle (*Veh*) and soluble NL-2 extracellular domain at concentrations of 5000 nM (5  $\mu$ M), 100 nM, 10 nM, and 1 nM (last four columns on the right). *C*, inhibition curve depicting effect of varying concentrations of NL-2 (x axis) on rat islet insulin secretion rate (y axis). Half-maximal inhibition of insulin secretion ( $IC_{50}$ ) occurs at 9 nM. Data are the mean  $\pm$  S.E. (error bars) of quadruplicate samples and, in *A* and *B*, are normalized to unstimulated secretion and are representative of at least three separate experiments (\*,  $p < 0.05$ ; \*\*,  $p < 0.01$ ; \*\*\*,  $p < 0.001$ ).

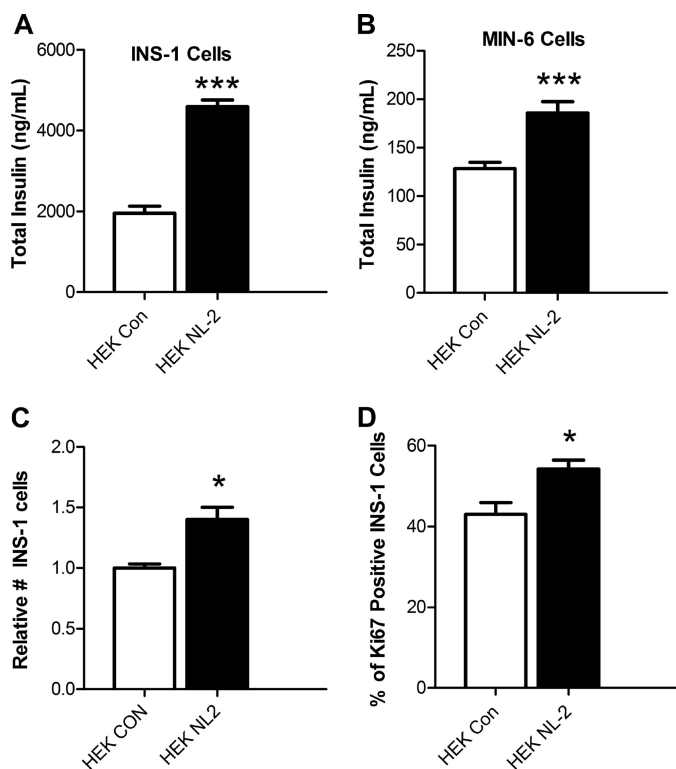


FIGURE 4. **Longer term co-culture with HEK293 cells expressing NL-2 increases cellular insulin content and INS-1 cell proliferation.** *A*, INS-1 cells were cultured for 48 h on monolayers of HEK293 cells transfected with full-length NL-2 (*HEK NL-2*) or with a control construct (*HEK Con*), and insulin levels in cell extracts were measured. *A* and *B*, insulin content of INS-1  $\beta$  cells (*A*) and MIN-6  $\beta$  cells (*B*) co-cultured with NL-2-expressing cells (black columns) or control-transfected cells (white columns). *C*, FACS analysis to count INS-1 (insulin-containing) cells showed that, after 48 h, there were  $\sim$ 50% more INS-1 cells in the NL-2 co-cultures (cell numbers shown normalized to number in control co-cultures). *D*, FACS analysis to determine the percentage of Ki67-positive INS-1 cells after 48 h of co-culture with NL-2-transfected HEK293 cells (black column) or with control-transfected HEK293 cells (white column) (\*,  $p < 0.05$ ; \*\*\*,  $p < 0.001$ ). Error bars, S.E.

$\beta$  cell-extracellular protein interactions are most likely to be intact and abundant, were employed. As can be seen in Fig. 5C, soluble NL-1-G500A, despite its inability to interact with neur-

exins, interfered with insulin secretion by rat islets. These data suggest that neurexin binding is unnecessary either for cell surface neuroligin to enhance insulin secretion or for soluble neuroligin to impair secretion.

These results demonstrate that NL-1 influences insulin secretion in a manner that does not require neurexin binding. Although unlikely, it is nonetheless possible that NL-2 and NL-1 enhance insulin secretion through divergent mechanisms and that the effect of NL-2, unlike that of NL-1, is exerted through neurexin. NL-2, however, has the lowest binding affinity of the neuroligins for neurexins (37). The structural basis for this low binding affinity has been described previously (18, 37, 40). Neuroligins interact with  $\alpha$ - and  $\beta$ -neurexins at the same site, which is highly similar between all three neurexins, near the carboxyl end of the neurexin extracellular domain (41, 42). Thus, the same neuroligin structural determinants promote or inhibit interactions with both  $\alpha$  and  $\beta$  forms of neurexin (40, 42). The extracellular domain of the  $\alpha$ -neurexins is extended N-terminal to the neuroligin-binding site. This extension hinders access to the neuroligin binding domain and reduces the affinity of  $\alpha$ -neurexins for neuroligin to  $\sim$ 2–3-fold below that of  $\beta$ -neurexins (42).

Whereas the  $K_d$  for the association between NL-1 and neurexin-1 $\beta$  is in the nanomolar range ( $\sim$ 29 nM), the  $K_d$  for NL-2 is in the micromolar range ( $\sim$ 8.8  $\mu$ M) (17). This affinity was previously determined by surface plasmon resonance binding analysis using immobilized glutathione *S*-transferase-fused neurexin (17). The neurexin fusion protein used was produced in bacteria and therefore not glycosylated. To further confirm the low affinity for neurexin predicted by the structure of NL-2, we repeated the prior surface plasmon resonance analysis using a well characterized, normally glycosylated IgG-neurexin construct (supplemental Fig. S2). As before, the affinity of NL-2 for neurexin was relatively low, with a  $K_d$  in the micromolar range (11.2  $\mu$ M) (supplemental Fig. S2). In contrast, the affinity of NL-2 for the  $\beta$  cell surface ( $K_b$ ; Fig. 1C) and the one-half maximal NL-2 concentration for reduction of insulin secretion



## Transcellular Neuroigin-2 Interactions in $\beta$ Cell Function

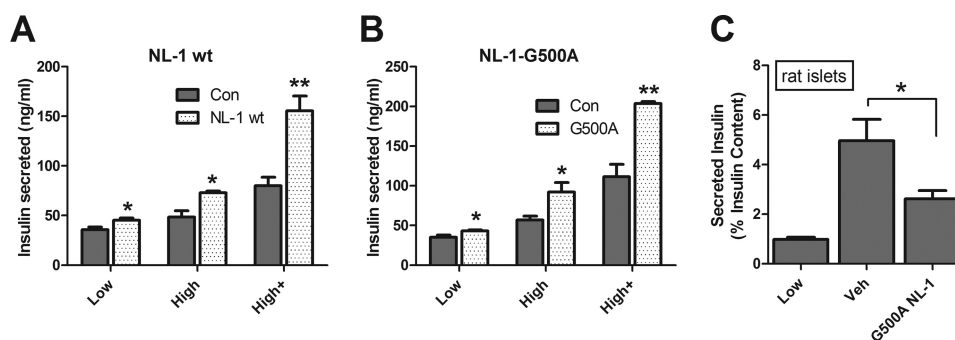


**FIGURE 5. Neurexin binding is not necessary for NL-1 to affect insulin secretion.** *A*, INS-1  $\beta$  cells were co-cultured with HEK293 cells transfected with neuroigin-1 (NL-1 wt, lighter columns) or with a control construct (Con, darker columns). Insulin secretion was measured after 1 h in 3 mM glucose (Low), 16.75 mM glucose (High), or 16.75 mM glucose plus 100  $\mu$ M IBMX (High+). In *B*, co-culture was with HEK293 cells expressing NL-1 with a Gly to Ala mutation at residue 500, which prevents neurexin binding (NL-1-G500A; lighter columns). Otherwise, the experiment was the same as in *A*. *C*, measurement of insulin secretion by intact rat islets incubated for 1 h at low (3 mM) glucose or at high (20 mM) glucose with either NaCl-HEPES vehicle alone (Veh; middle column) or recombinant soluble NL-1-G500A (5  $\mu$ M, rightmost column) (\*,  $p < 0.05$ ; \*\*,  $p < 0.01$ ). Error bars, S.E.

(IC<sub>50</sub>; Fig. 3C) were both  $\leq 15$  nM, more than 700-fold lower than would be expected if neurexin-NL-2 binding were mediating these effects (based on the  $K_d$  from supplemental Fig. S2).

**The Effect of NL-2 on Insulin Secretion Occurs Distal to Glucose Sensing**—Neuroigin increases neurotransmitter secretion by driving assembly of presynaptic protein complexes that mediate regulated exocytosis (11). Given the similarities between the synaptic and  $\beta$  cell secretory machineries, neuroigin probably exerts its effect on insulin secretion in a parallel manner, by enhancing function of the insulin secretory machinery, therefore acting downstream of glucose sensing. To test whether NL-2 increases insulin secretion via an effect distal to the  $\beta$  cell glucose-sensing mechanism, we asked whether stimulation of insulin secretion by forced  $\beta$  cell depolarization rather than by glucose would abrogate the NL-2 effect. In co-cultures with NL-2, insulin secretion driven by KCl-mediated depolarization was still increased, indicating that the effect of NL-2 occurs downstream of glucose sensing (Fig. 6A).

The functional equivalent of the presynaptic active sites of secretion in  $\beta$  cells are microdomains (alternatively referred to as “excitosomes,” “Ca<sup>2+</sup> microdomains,” or “secretory microdomains”), where the submembrane secretory apparatus assembles beneath the plasma membrane in close proximity to voltage-gated calcium channels (43–46). Because these microdomains seem to be especially important for early phase insulin secretion, we next asked whether NL-2 affected early phase insulin secretion more than late phase (47–49). Drawing on prior studies analyzing early and late phase insulin secretion in INS-1 cells (50–53), we compared the magnitude of the effect of NL-2 on early and late phase insulin secretion by INS-1 cells by comparing the rates of insulin secretion for the first 10 min and the next 50 min after high glucose stimulation (Fig. 6B). During the period of early insulin secretion, exposure to HEK293 cells synthesizing NL-2 increased insulin secretion 1.7-fold over secretion in the control co-culture (Fig. 6B, compare columns 5 and 6). In contrast, the increase in late phase secretion in the NL-2 co-cultures compared with the control co-cultures was not statistically significant (Fig. 6B, compare columns 7 and 8).

**NL-2 Affects Secretory Microdomain Assembly and/or Function**—The voltage-dependent calcium channels that mediate the triggering of insulin exocytosis are few in number

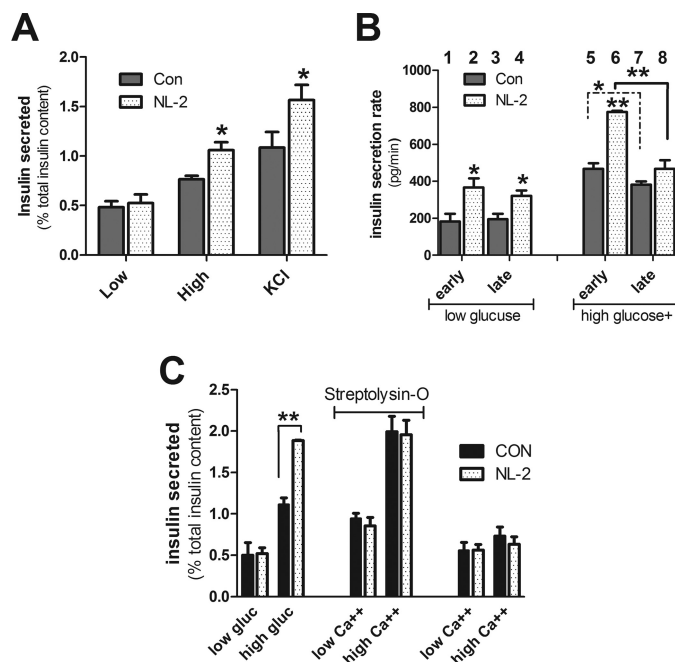


**FIGURE 6. Extracellular NL-2 interactions affect insulin secretion distal to glucose sensing.** *A*, INS-1 cells were co-cultured for 24 h with NL-2-transfected HEK293 cells (lighter columns) or control-transfected HEK293 cells (darker columns). Insulin secretion (as a percentage of total insulin content) was measured at 3 mM glucose (Low) or 20 mM glucose (High) or after direct stimulation with 30 mM KCl. *B*, INS-1 cells were co-cultured for 24 h as in *A*. After a 45-min preincubation at 3 mM glucose, their rate of insulin secretion into the medium was assessed for the first 10 min (early) and the next 50 min (late) after being switched into fresh medium with either 3 mM glucose (low glucose) or 20 mM glucose with IBMX (high glucose+). Asterisks immediately above the columns from the NL-2 co-cultures indicate significantly increased secretion relative to the control co-culture result in the adjacent column to the left. *C*, INS-1 cells were co-cultured as in *A* and *B*. In the left four columns, insulin secretion at high and low glucose was measured as in *A* but for 15 min instead of 1 h. In the remaining columns, insulin secretion was measured after a 15-min incubation in medium with 0.1  $\mu$ M free calcium (low Ca<sup>++</sup>) or with 10  $\mu$ M free calcium (high Ca<sup>++</sup>). The last four columns on the right confirm that higher free calcium alone did not stimulate insulin secretion in non-permeabilized cells. The center four columns show insulin secretion by cells first permeabilized with streptolysin-O (\*,  $p < 0.05$ ; \*\*,  $p < 0.01$ ). Error bars, S.E.

in  $\beta$  cells and localize to the secretory microdomains in order to be in close proximity to the exocytic machinery (43–46). Ca<sup>2+</sup> entry after stimulation occurs preferentially at these sites. To test whether the effect of NL-2 on insulin exocytosis would still be evident if Ca<sup>2+</sup> influx occurred elsewhere (outside of the

secretory microdomains), insulin secretion after  $\text{Ca}^{2+}$  entry through experimentally induced pores in the  $\beta$  cell membrane was measured. In INS-1 cells permeabilized by streptolysin-O treatment, high  $\text{Ca}^{2+}$ , as expected, triggered insulin release. The increased insulin secretion normally seen after co-culture with NL-2-expressing HEK293 cells, however, was abolished (Fig. 6C).

We next asked whether NL-2, analogous to its role in inducing assembly of the presynaptic secretory machinery in axonal nerve terminals, enhances  $\beta$  cell secretory microdomain assembly. Secretory microdomain assembly includes submembrane localization and clustering of t-SNAREs, such as syntaxin-1A, and other exocytic proteins (49, 54, 55). Neuroligin-induced assembly of the active zones of exocytosis in neuronal processes can be quantitatively assessed by analysis of presynaptic secretory protein clustering (27–29). As has been described, secretory protein clustering is reflected by the punctateness (intensity distribution) of secretory protein immunofluorescent staining; increased protein clustering increases the intensity of the immunofluorescent signal at the punctate sites of staining representing clustered proteins (27–29). We adapted this approach, as illustrated in supplemental Fig. S3, to assess syntaxin-1A clustering in co-cultured INS-1  $\beta$  cells. Transfection of HEK293 cells with NL-2 or with a control protein yielded confluent lawns of HEK293 cells with regional variation in the fraction of successfully transfected cells (Fig. 7A and supplemental Fig. S3). After a 24-h period of co-culture, syntaxin-1A, present in the INS-1  $\beta$  cells but not the HEK293 cells, was detected by immunofluorescence (Fig. 7B). As in prior studies of neuroligin function assessing presynaptic synapsin clustering (27, 29), the immunofluorescent signal intensity of syntaxin-1A-positive sites was measured (Fig. 7C). The area covered by HEK293 cells expressing transfected protein was measured at the same time. In the NL-2 co-cultures, the mean syntaxin-1A intensity in any given region within a culture dish increased proportionally with the extent of NL-2 expression by the HEK293 cells within that region (Fig. 7E; see also supplemental Fig. S3). This relationship was absent in the control co-cultures; changes in the proportion of HEK293 cells expressing the control protein did not affect the mean syntaxin-1A intensity (Fig. 7F). Furthermore, an increase in overall mean syntaxin-1A intensity was detected in NL-2 co-cultures as compared with control co-cultures (Fig. 7D). This increase was significant, although its magnitude may have been blunted by the limited surface area of the INS-1 cells that came directly into contact with the NL-2-expressing HEK293 cells.

Changes in microdomain formation induced by contact with NL-2-expressing cells could affect the number of insulin granules docked at the  $\beta$  cell membrane. The co-culture system, however, is not amenable to EM, which would be necessary to analyze insulin granule docking, and it would be very challenging, in any case, to identify sites on electron micrographs where  $\beta$  cells and transfected HEK293 cells came into contact. Instead, to test whether altered NL-2 expression affects insulin granule docking, we analyzed granule docking in islets from NL-2 knock-out mice (supplemental Fig. S4; a more complete investigation of the effect of NL-2 knockout on islet function is pending) (32). Using EM, we found that the proportion of

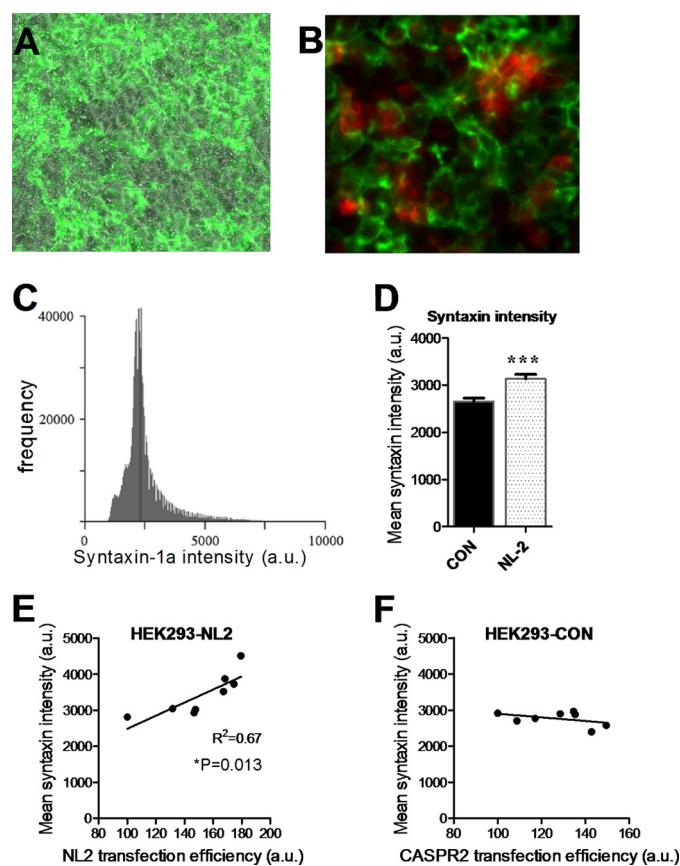


**FIGURE 7. NL-2 promotes syntaxin-1A clustering (see supplemental Fig. S3 for illustration of approach).** A, lawns of HEK293 cells were prepared for co-culture by transient transfection with either NL-2 or, as a control, with CASPR2, a different neuronal (non-synaptic) plasma membrane protein. Both proteins carry FLAG epitope tags. An example of a typical HEK293 cell lawn after transient transfection (in this case with NL-2) is shown. The cells that were successfully transfected were detected by immunofluorescent staining with an anti-FLAG antibody. A bright field image ( $\times 20$ ) and the corresponding image of the immunofluorescent staining (green) are shown merged. Non-transfected HEK293 cells are translucent and more difficult to see. They are present wherever there is no immunofluorescent signal. B, dispersed INS-1  $\beta$  cells were co-cultured with the HEK293 cells. An example is shown. Staining was with an anti-FLAG antibody to detect transfected HEK293 cells (green) and with an antibody against the  $\beta$  cell protein syntaxin-1A (red;  $\times 60$ ). In the examples shown in A and B, the HEK293 cells have been transfected with NL-2. Images from control co-cultures with CASPR2 appear qualitatively identical. C, an example of a histogram generated from measuring the signal intensity in syntaxin-1A-positive pixels (in arbitrary units (a.u.)). D, mean INS-1 cell syntaxin-1A intensity after a 24-h co-culture with control-transfected cells (black column) or NL-2-transfected cells (gray column). E and F, eight randomly selected regions per culture dish were imaged. Mean syntaxin-1A immunofluorescence intensity (y axis) was plotted against transfection efficiency in that region as represented by the area covered by successfully transfected cells (cell area positive for staining with the anti-FLAG antibody; x axis). In E, in which INS-1 cells were co-cultured with HEK293 cells transfected to express NL-2, mean syntaxin-1A intensity increased with local transfection efficiency. The slope of the derived line was positive (the slope was non-zero, indicating that the local mean syntaxin-1A staining intensity varied with the local NL-2-positive area;  $p = 0.013$ ). In F, with control-transfected HEK293 cells, there was no relationship between syntaxin-1A staining and HEK293 cell transfection efficiency. Data in E and F are representative of independent analysis of three culture wells for each condition, with NL-2 yielding a positive association in each well and the control protein, CASPR2, yielding no association. The experiment was repeated with same outcome on three separate occasions (\*\*\*,  $p < 0.001$ ). Error bars, S.E.

docked insulin granules was reduced by 33% in NL-2 KO  $\beta$  cells with no change in mean granule number per cell or granule density (Fig. S4).



### DISCUSSION

These experiments demonstrate that extracellular NL-2 interactions play an integral role in  $\beta$  cell function. Together with our prior findings regarding NL-2, particularly that NL-2 overexpression increases and knockdown decreases insulin secretion by rat islet and INS-1  $\beta$  cells (14), this study reveals for the first time that NL-2 helps guide secretory function at a tissue site other than the CNS. As in the synapse, NL-2 functions via a transcellular mechanism, providing a means by which  $\beta$  cells can influence the insulin secretory function of other, neighboring  $\beta$  cells. NL-2 in the CNS interacts with proteins across the synaptic cleft to promote and maintain assembly of the presynaptic exocytic machinery (11–13). Our results are consistent with NL-2 similarly acting in a transcellular manner to promote the assembly of submembrane secretory sites in  $\beta$  cells.

As in neurons, transcellular neuroligin activity is dependent on neuroligin being presented on a cell surface, most likely in a clustered fashion, rather than free in solution. Treatment of  $\beta$  cells with soluble NL-2 impaired insulin secretion. This result parallels the outcomes of similar experiments in neuronal co-cultures, in which the addition of soluble proteins to the culture media disrupted endogenous neuroligin interactions and inhibited synaptogenesis (12, 13, 29). NL-2 binds to a partner on the  $\beta$  cell surface with nanomolar affinity. As would be expected if this binding interaction were responsible for the effect of NL-2 on insulin secretion, the concentration of half-maximal binding ( $K_d \sim 15$  nM) was approximately the same as the concentration at which half-maximal inhibition of insulin secretion occurred ( $IC_{50} \sim 9$  nM).

In the CNS, neuroligins exert their effects in both a neurexin-dependent and neurexin-independent fashion (36). Although  $\beta$  cells express neurexin (14, 16), the increased insulin secretion brought about by neuroligin is probably not dependent on neurexin binding. Two observations provide evidence for this. First, NL-1 mutated to prevent neurexin binding can nevertheless drive increased insulin secretion in co-culture or, in soluble form, disrupt the endogenous neuroligin interactions that facilitate insulin secretion. Second, the affinity of NL-2 for neurexin is low, with a  $K_d$  much higher than either the  $IC_{50}$  of the soluble NL-2 affect on insulin secretion or the observed  $K_d$  for the binding of NL-2 to the  $\beta$  cell surface. This suggests that the effect of NL-2 on insulin secretion is driven by a binding interaction of much higher affinity than that associated with NL-2-neurexin binding.

We recently showed that neurexin-1 $\alpha$  is essential for insulin granule docking and that decreased neurexin expression increases insulin secretion (16). Because of this, experiments directly probing the role of NL-2-neurexin interactions by knocking down neurexin would be confounded by the resulting defects in secretory granule docking and abnormally elevated insulin secretion. Also, because  $\beta$  cells express extracellular neurexin binding partners other than neuroligin, we would have been unable to attribute any effects caused by incubation of  $\beta$  cells with soluble neurexin or by neurexin knockdown specifically to interference with neuroligin-neurexin interactions (16).

Our interest in NL-2 was sparked by the observation that in neuronal co-cultures, NL-2 drives assembly of the presynaptic active zone (11, 29). Of particular interest, NL-2 induces specifically *inhibitory* synapse formation. This is significant because  $\beta$  cells express unique inhibitory synaptic proteins and contain the major inhibitory neurotransmitter GABA (11, 56, 57). It is tempting to speculate that the presence of inhibitory synaptic proteins in  $\beta$  cells is due to an influence of NL-2 on  $\beta$  cell maturation. Further work will be necessary to determine the role of NL-2 in  $\beta$  cell differentiation.

Overall, our findings reveal that our hypothesis that NL-2 functions in a transcellular manner in  $\beta$  cells is correct, adding to our understanding of why  $\beta$  cell- $\beta$  cell contact enhances insulin secretion. Subsets of neuroligins and neurexins are reportedly also expressed within the vascular system (58). Although we did not observe these proteins in pancreatic tissue outside of the  $\beta$  cells, it is nevertheless possible that they may also be present in islet capillaries and hence able to mediate interactions between the islet vasculature and  $\beta$  cells (14). In addition to enhancing insulin secretion, longer exposure to NL-2 increased INS-1  $\beta$  cell, but not primary rat islet  $\beta$  cell, proliferation. The significance of this effect on proliferation is uncertain.

The increases in insulin secretion observed in the co-culture experiments were probably limited by the extent of cell-cell contact that could be achieved by placing dispersed  $\beta$  cells into contact with a monolayer of HEK293 cells. Contacting more of the  $\beta$  cell surface with NL-2 may have resulted in greater increases in insulin secretion. The extent of  $\beta$  cell contact with NL-2-expressing cells was also limited by the necessity of using transient transfection to induce NL-2 expression (an adequate stably transfected line could not be generated). Transient transfection efficiencies (percentage of cells transfected) were always less than 100%, further limiting contact of  $\beta$  cells with HEK293 cell surface NL-2 (59).

The  $\beta$  cell surface secretory microdomains are sites where t-SNARE protein assemblies preferentially localize and where the highest levels of stimulatory  $Ca^{2+}$  influx and first phase insulin release occur (43–46). The  $\beta$  cell secretory microdomains can be thought of as the functional equivalent of the presynaptic active zone. This analogy is strengthened by the evidence we have presented here indicating that secretory microdomain formation and/or function, like that of the presynaptic active zone, is enhanced by transcellular neuroligin interactions. There may be other, as yet unidentified, membrane domains that serve as the equivalent of postsynaptic sites. The presence of  $\beta$  cell presynaptic-like and postsynaptic-like plasma membrane domains would allow segregation of neuroligin from its extracellular binding partner(s), thus facilitating transcellular interactions. That EphA5 and ephrin-A5 segregate to separate sites on the  $\beta$  cell membrane is evidence that such discrete domains exist (7).

In summary, these results show that neuroligin engages in transcellular interactions that enhance insulin secretion by  $\beta$  cells. Our findings suggest that the close parallels that exist between the  $\beta$  cell and synaptic secretory machineries extend beyond the well studied sub-plasma membrane secretory protein complexes and into extracellular sites of  $\beta$  cell- $\beta$  cell con-

tact. Extracellular NL-2 interactions help determine  $\beta$  cell insulin secretory capacity, probably stabilizing and/or promoting the assembly of the secretory machinery within the  $\beta$  cell secretory microdomains. Our data suggest that interaction with neurexin is not necessary in order for neuroligin to increase insulin secretion. If protein-protein interactions between  $\beta$  cells resemble those across the synaptic cleft, other extracellular protein interactions affecting insulin secretion will most likely be found. Future studies are needed to elucidate whether neuroligin plays a role in  $\beta$  cell differentiation and whether neuroligin or downstream molecules might be useful targets for treating the impaired insulin secretion associated with diabetes.

*Acknowledgments*—We thank Ying Jones for assistance with electron microscopy preparation, Dr. M. Farquhar for use of the Cellular and Molecular Medicine Electron Microscopy Facility, and Frédérique Varoqueaux for generously providing the mice used in the EM study. We thank Brittany Russell for invaluable assistance with analysis of electron micrographs.

## REFERENCES

- Jain, R., and Lammert, E. (2009) Cell-cell interactions in the endocrine pancreas. *Diabetes Obes. Metab.* **11**, Suppl. 4, 159–167
- Hauge-Evans, A. C., Squires, P. E., Persaud, S. J., and Jones, P. M. (1999) Pancreatic  $\beta$  cell-to- $\beta$  cell interactions are required for integrated responses to nutrient stimuli. Enhanced  $\text{Ca}^{2+}$  and insulin secretory responses of MIN6 pseudoislets. *Diabetes* **48**, 1402–1408
- Chen, W., Begum, S., Opere-Addo, L., Garyu, J., Gibson, T. F., Bothwell, A. L., Papaioannou, V. E., and Herold, K. C. (2009) Promotion of  $\beta$  cell differentiation in pancreatic precursor cells by adult islet cells. *Endocrinology* **150**, 570–579
- Ravier, M. A., Güldenagel, M., Charollais, A., Gjinovci, A., Caille, D., Söhl, G., Wollheim, C. B., Willecke, K., Henquin, J. C., and Meda, P. (2005) Loss of connexin36 channels alters  $\beta$  cell coupling, islet synchronization of glucose-induced  $\text{Ca}^{2+}$  and insulin oscillations, and basal insulin release. *Diabetes* **54**, 1798–1807
- Kelly, C., McClenaghan, N. H., and Flatt, P. R. (2011) Role of islet structure and cellular interactions in the control of insulin secretion. *Islets* **3**, 41–47
- Bosco, D., Haefliger, J. A., and Meda, P. (2011) Connexins. Key mediators of endocrine function. *Physiol. Rev.* **91**, 1393–1445
- Konstantinova, I., Nikolova, G., Ohara-Imaizumi, M., Meda, P., Kucera, T., Zarbalis, K., Wurst, W., Nagamatsu, S., and Lammert, E. (2007) EphA-Ephrin-A-mediated  $\beta$  cell communication regulates insulin secretion from pancreatic islets. *Cell* **129**, 359–370
- Esní, F., Täljedal, I. B., Perl, A. K., Cremer, H., Christofori, G., and Semb, H. (1999) Neural cell adhesion molecule (N-CAM) is required for cell type segregation and normal ultrastructure in pancreatic islets. *J. Cell Biol.* **144**, 325–337
- Jaques, F., Jousset, H., Tomas, A., Prost, A. L., Wollheim, C. B., Irminger, J. C., Demaurex, N., and Halban, P. A. (2008) Dual effect of cell-cell contact disruption on cytosolic calcium and insulin secretion. *Endocrinology* **149**, 2494–2505
- Easom, R. A. (2000)  $\beta$  Granule transport and exocytosis. *Semin. Cell Dev. Biol.* **11**, 253–266
- Craig, A. M., and Kang, Y. (2007) Neurexin-neuroligin signaling in synapse development. *Curr. Opin. Neurobiol.* **17**, 43–52
- Graf, E. R., Zhang, X., Jin, S. X., Linhoff, M. W., and Craig, A. M. (2004) Neurexins induce differentiation of GABA and glutamate postsynaptic specializations via neuroligins. *Cell* **119**, 1013–1026
- Dean, C., Scholl, F. G., Choih, J., DeMaria, S., Berger, J., Isacoff, E., and Scheiffele, P. (2003) Neurexin mediates the assembly of presynaptic terminals. *Nat. Neurosci.* **6**, 708–716
- Suckow, A. T., Comoletti, D., Waldrop, M. A., Mosedale, M., Egodage, S., Taylor, P., and Chessler, S. D. (2008) Expression of neurexin, neuroligin, and their cytoplasmic binding partners in the pancreatic  $\beta$  cells and the involvement of neuroligin in insulin secretion. *Endocrinology* **149**, 6006–6017
- Maffei, A., Liu, Z., Witkowski, P., Moschella, F., Del Pozzo, G., Liu, E., Herold, K., Winchester, R. J., Hardy, M. A., and Harris, P. E. (2004) Identification of tissue-restricted transcripts in human islets. *Endocrinology* **145**, 4513–4521
- Mosedale, M., Egodage, S., Calma, R. C., Chi, N. W., and Chessler, S. D. (2012) Neurexin-1 $\alpha$  contributes to insulin-containing secretory granule docking. *J. Biol. Chem.* **287**, 6350–6361
- Comoletti, D., Flynn, R. E., Boucard, A. A., Demeler, B., Schirf, V., Shi, J., Jennings, L. L., Newlin, H. R., Südhof, T. C., and Taylor, P. (2006) Gene selection, alternative splicing, and post-translational processing regulate neuroligin selectivity for  $\beta$ -neurexins. *Biochemistry* **45**, 12816–12827
- Leone, P., Comoletti, D., Ferracci, G., Conrod, S., Garcia, S. U., Taylor, P., Bourne, Y., and Marchot, P. (2010) Structural insights into the exquisite selectivity of neurexin/neuroligin synaptic interactions. *EMBO J.* **29**, 2461–2471
- Jungers, J., Delogne-Desnoeck, J., and Robyn, C. (1981) A simple and rapid solid-phase radioimmunoassay for serum progesterone, using the protein A of *Staphylococcus aureus* as immunoadsorbent. *J. Lab. Clin. Med.* **98**, 30–36
- Papadimitriou, J. M., and van Duijn, P. (1970) Effects of fixation and substrate protection on the isoenzymes of aspartate aminotransferase studied in a quantitative cytochemical model system. *J. Cell Biol.* **47**, 71–83
- De Jaco, A., Comoletti, D., Kovarik, Z., Gaietta, G., Radic, Z., Lockridge, O., Ellisman, M. H., and Taylor, P. (2006) A mutation linked with autism reveals a common mechanism of endoplasmic reticulum retention for the  $\alpha$ , $\beta$ -hydrolase fold protein family. *J. Biol. Chem.* **281**, 9667–9676
- Sweet, I. R., Cook, D. L., Lernmark, A., Greenbaum, C. J., Wallen, A. R., Marcum, E. S., Stekhova, S. A., and Krohn, K. A. (2004) Systematic screening of potential  $\beta$  cell imaging agents. *Biochem. Biophys. Res. Commun.* **314**, 976–983
- Kenakin, T. P. (2006) *A Pharmacology Primer: Theory, Applications, and Methods*, 2nd Ed. pp. 59–78, Academic Press/Elsevier, Amsterdam
- Deeney, J. T., Gromada, J., Høy, M., Olsen, H. L., Rhodes, C. J., Prentki, M., Berggren, P. O., and Corkey, B. E. (2000) Acute stimulation with long chain acyl-CoA enhances exocytosis in insulin-secreting cells (HIT T-15 and NMRI  $\beta$  cells). *J. Biol. Chem.* **275**, 9363–9368
- Thurmond, D. C., Gonelle-Gispert, C., Furukawa, M., Halban, P. A., and Pessin, J. E. (2003) Glucose-stimulated insulin secretion is coupled to the interaction of actin with the t-SNARE (target membrane soluble N-ethylmaleimide-sensitive factor attachment protein receptor protein) complex. *Mol. Endocrinol.* **17**, 732–742
- Deeney, J. T., Bränström, R., Corkey, B. E., Larsson, O., and Berggren, P. O. (2007)  $^3\text{H}$ -Serotonin as a marker of oscillatory insulin secretion in clonal  $\beta$  cells (INS-1). *FEBS Lett.* **581**, 4080–4084
- Shi, P., Scott, M. A., Ghosh, B., Wan, D., Wissner-Gross, Z., Mazitschek, R., Haggarty, S. J., and Yanik, M. F. (2011) Synapse microarray identification of small molecules that enhance synaptogenesis. *Nat. Commun.* **2**, 510
- Wooding, S., and Pelham, H. R. (1998) The dynamics of Golgi protein traffic visualized in living yeast cells. *Mol. Biol. Cell* **9**, 2667–2680
- Scheiffele, P., Fan, J., Choih, J., Fetter, R., and Serafini, T. (2000) Neuroligin expressed in nonneuronal cells triggers presynaptic development in contacting axons. *Cell* **101**, 657–669
- Asfari, M., Janjic, D., Meda, P., Li, G., Halban, P. A., and Wollheim, C. B. (1992) Establishment of 2-mercaptoethanol-dependent differentiated insulin-secreting cell lines. *Endocrinology* **130**, 167–178
- Spies, Y., Smith, M. A., and Vale, W. (1982) Superfusion of dissociated pancreatic islet cells attached to Cytodex beads. *Diabetes* **31**, 189–193
- Varoqueaux, F., Aramuni, G., Rawson, R. L., Mohrmann, R., Missler, M., Gottmann, K., Zhang, W., Südhof, T. C., and Brose, N. (2006) Neuroligins determine synapse maturation and function. *Neuron* **51**, 741–754
- Levinson, J. N., Chéry, N., Huang, K., Wong, T. P., Gerrow, K., Kang, R., Prange, O., Wang, Y. T., and El-Husseini, A. (2005) Neuroligins mediate excitatory and inhibitory synapse formation. Involvement of PSD-95 and neurexin-1 $\beta$  in neuroligin-induced synaptic specificity. *J. Biol. Chem.* **280**,

## Transcellular Neuroligin-2 Interactions in $\beta$ Cell Function

- 17312–17319
34. Gerdes, J., Lemke, H., Baisch, H., Wacker, H. H., Schwab, U., and Stein, H. (1984) Cell cycle analysis of a cell proliferation-associated human nuclear antigen defined by the monoclonal antibody Ki-67. *J. Immunol.* **133**, 1710–1715
  35. Zucker, R. M., Elstein, K. H., Easterling, R. E., and Massaro, E. J. (1988) Flow cytometric discrimination of mitotic nuclei by right-angle light scatter. *Cytometry* **9**, 226–231
  36. Ko, J., Zhang, C., Arac, D., Boucard, A. A., Brunger, A. T., and Südhof, T. C. (2009) Neuroligin-1 performs neurexin-dependent and neurexin-independent functions in synapse validation. *EMBO J.* **28**, 3244–3255
  37. Chen, X., Liu, H., Shim, A. H., Focia, P. J., and He, X. (2008) Structural basis for synaptic adhesion mediated by neuroligin-neurexin interactions. *Nat. Struct. Mol. Biol.* **15**, 50–56
  38. Reissner, C., Klose, M., Fairless, R., and Missler, M. (2008) Mutational analysis of the neurexin-neuroligin complex reveals essential and regulatory components. *Proc. Natl. Acad. Sci. U.S.A.* **105**, 15124–15129
  39. Ichtchenko, K., Nguyen, T., and Südhof, T. C. (1996) Structures, alternative splicing, and neurexin binding of multiple neuroligins. *J. Biol. Chem.* **271**, 2676–2682
  40. Fabrichny, I. P., Leone, P., Sulzenbacher, G., Comoletti, D., Miller, M. T., Taylor, P., Bourne, Y., and Marchot, P. (2007) Structural analysis of the synaptic protein neuroligin and its  $\beta$ -neurexin complex. Determinants for folding and cell adhesion. *Neuron* **56**, 979–991
  41. Koehnke, J., Jin, X., Trbovic, N., Katsamba, P. S., Brasch, J., Ahlsen, G., Scheiffele, P., Honig, B., Palmer, A. G., 3rd, and Shapiro, L. (2008) Crystal structures of  $\beta$ -neurexin 1 and  $\beta$ -neurexin 2 ectodomains and dynamics of splice insertion sequence 4. *Structure* **16**, 410–421
  42. Miller, M. T., Mileni, M., Comoletti, D., Stevens, R. C., Harel, M., and Taylor, P. (2011) The crystal structure of the  $\alpha$ -neurexin-1 extracellular region reveals a hinge point for mediating synaptic adhesion and function. *Structure* **19**, 767–778
  43. Leung, Y. M., Kwan, E. P., Ng, B., Kang, Y., and Gaisano, H. Y. (2007) SNAREing voltage-gated  $K^+$  and ATP-sensitive  $K^+$  channels. Tuning  $\beta$  cell excitability with syntaxin-1A and other exocytotic proteins. *Endocr. Rev.* **28**, 653–663
  44. Rutter, G. A., Tsuboi, T., and Ravier, M. A. (2006)  $Ca^{2+}$  microdomains and the control of insulin secretion. *Cell Calcium* **40**, 539–551
  45. Wisner, O., Trus, M., Hernández, A., Renström, E., Barg, S., Rorsman, P., and Atlas, D. (1999) The voltage sensitive Lc-type  $Ca^{2+}$  channel is functionally coupled to the exocytotic machinery. *Proc. Natl. Acad. Sci. U.S.A.* **96**, 248–253
  46. Ohara-Imaizumi, M., Nishiwaki, C., Kikuta, T., Kumakura, K., Nakamichi, Y., and Nagamatsu, S. (2004) Site of docking and fusion of insulin secretory granules in live MIN6  $\beta$  cells analyzed by TAT-conjugated anti-syntaxin 1 antibody and total internal reflection fluorescence microscopy. *J. Biol. Chem.* **279**, 8403–8408
  47. Barg, S., Eliasson, L., Renstrom, E., and Rorsman, P. (2002) *Diabetes* **51**, Suppl. 1, S74–S82
  48. Barg, S., Ma, X., Eliasson, L., Galvanovskis, J., Göpel, S. O., Obermüller, S., Platzer, J., Renström, E., Trus, M., Atlas, D., Striessnig, J., and Rorsman, P. (2001) Fast exocytosis with few  $Ca^{2+}$  channels in insulin-secreting mouse pancreatic B cells. *Biophys. J.* **81**, 3308–3323
  49. Ohara-Imaizumi, M., Fujiwara, T., Nakamichi, Y., Okamura, T., Akimoto, Y., Kawai, J., Matsushima, S., Kawakami, H., Watanabe, T., Akagawa, K., and Nagamatsu, S. (2007) Imaging analysis reveals mechanistic differences between first- and second-phase insulin exocytosis. *J. Cell Biol.* **177**, 695–705
  50. Ivarsson, R., Jing, X., Waselle, L., Regazzi, R., and Renström, E. (2005) Myosin 5a controls insulin granule recruitment during late-phase secretion. *Traffic* **6**, 1027–1035
  51. Li, J., Luo, R., Kowluru, A., and Li, G. (2004) Novel regulation by Rac1 of glucose- and forskolin-induced insulin secretion in INS-1  $\beta$  cells. *Am. J. Physiol. Endocrinol. Metab.* **286**, E818–E827
  52. Marshall, C., Hitman, G. A., Partridge, C. J., Clark, A., Ma, H., Shearer, T. R., and Turner, M. D. (2005) Evidence that an isoform of calpain-10 is a regulator of exocytosis in pancreatic  $\beta$  cells. *Mol. Endocrinol.* **19**, 213–224
  53. Straub, S. G., and Sharp, G. W. (2002) Glucose-stimulated signaling pathways in biphasic insulin secretion. *Diabetes Metab. Res. Rev.* **18**, 451–463
  54. Aoyagi, K., Ohara-Imaizumi, M., and Nagamatsu, S. (2011) Regulation of resident and newcomer insulin granules by calcium and SNARE proteins. *Front. Biosci.* **16**, 1197–1210
  55. Lang, T., Bruns, D., Wenzel, D., Riedel, D., Holroyd, P., Thiele, C., and Jahn, R. (2001) SNAREs are concentrated in cholesterol-dependent clusters that define docking and fusion sites for exocytosis. *EMBO J.* **20**, 2202–2213
  56. Suckow, A. T., Craige, B., Faundez, V., Cain, W. J., and Chessler, S. D. (2010) An AP-3-dependent mechanism drives synaptic-like microvesicle biogenesis in pancreatic islet  $\beta$  cells. *Am. J. Physiol. Endocrinol. Metab.* **299**, E23–E32
  57. Chessler, S. D., Simonson, W. T., Sweet, I. R., and Hammerle, L. P. (2002) Expression of the vesicular inhibitory amino acid transporter in pancreatic islet cells. Distribution of the transporter within rat islets. *Diabetes* **51**, 1763–1771
  58. Bottos, A., Destro, E., Rissone, A., Graziano, S., Cordara, G., Assenzio, B., Cera, M. R., Mascia, L., Bussolino, F., and Arese, M. (2009) The synaptic proteins neurexins and neuroligins are widely expressed in the vascular system and contribute to its functions. *Proc. Natl. Acad. Sci. U.S.A.* **106**, 20782–20787
  59. Dalby, B., Cates, S., Harris, A., Ohki, E. C., Tilkins, M. L., Price, P. J., and Ciccarone, V. C. (2004) Advanced transfection with Lipofectamine 2000 reagent. Primary neurons, siRNA, and high-throughput applications. *Methods* **33**, 95–103